Inorganic Chemistry

Article

pubs.acs.org/IC

Electrochemical Illumination of Intramolecular Communication in Ferrocene-Containing *tris*-*β*-Diketonato Aluminum(III) Complexes; Cytotoxicity of $Al(FcCOCHCOCF_3)_3$

Henno J. Gericke, Alfred J. Muller,† and Jannie C. Swarts*

Department of Chemistry, University of the Free State, P.O. Box 339, Bloemfontein, 9300, Republic of South Africa

Ⓢ *Supporting Information*

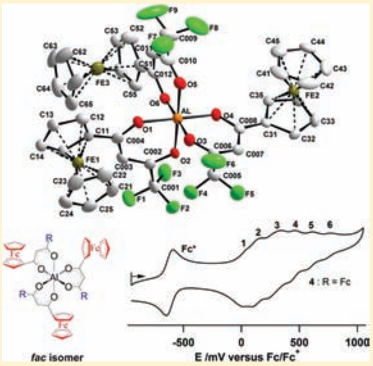

ABSTRACT: The series of ferrocene-containing *tris*-*β*-diketonato aluminum(III) complexes $[Al(FcCOCHCOR)_3]$ (R = CF_3, **1**; CH_3, **2**; C_6H_5, **3**; and Fc = ferrocenyl = $Fe(\eta^5\text{-}C_5H_5)(\eta^5\text{-}C_5H_4)$, **4**) were synthesized and investigated structurally and electrochemically; complex **1** was subjected to cytotoxicity tests. ^1H NMR-spectroscopy distinguished between the *mer* and *fac* isomers of **2** and **3**. Complex **1** existed only as the *mer* isomer. A single crystal X-ray crystallographic determination of the structure of a *mer*-isomer of $Al(FcCOCHCOCF_3)_3$, **1**, ($Z = 4$, space group $P2_12_12_1$) demonstrated extensive delocalization of all bonds which explained the pronounced electrochemically observed intramolecular communication between molecular fragments. In contrast to electrochemical studies in $CH_2Cl_2/[N(^nBu)_4][PF_6]$, the use of the supporting electrolyte $[N(^nBu)_4][B(C_6F_5)_4]$ allowed identification of all Fc/Fc^+ electrochemical couples by cyclic and square wave voltammetry for **1**−**4**. For R = Fc, formal reduction potentials of the six ferrocenyl groups were found to be $E^{\circ\prime}$ = 33, 123, 304, 432, 583, and 741 mV versus free ferrocene respectively. Complex **1** (IC_{50} = 10.6 μmol dm^{-3}) was less cytotoxic than the free $FcCOCH_2COCF_3$ ligand having IC_{50} = 6.8 μmol dm^{-3} and approximately 2 orders of magnitude less toxic to human HeLa neoplastic cells than cisplatin (IC_{50} = 0.19 μmol dm^{-3}).

■ INTRODUCTION

Ferrocene and the ferrocenyl group in compounds are studied as donors in energy transfer processes,[1] because they enhance catalytic activity in many reactions,[2,3] as high-burning rate composite propellant catalyst,[4] as active component in anticancer drugs,[5] and as a strong electron-donating substituent to manipulate electron density on complexes.[3,6] They are often used in electron transfer processes[7] because of their high thermal stability, reversible redox behavior, and their chemical modification possibilities. We have recently reported the synthesis of a number of ferrocene-containing *β*-diketonato-rhodium(I) complexes,[3,8] as part of a program to establish how the ferrocenyl fragment will influence the reactivity of the rhodium nucleus in substitution[9] and oxidative addition reactions,[10] a reaction which is inter alia important in the carbonylation of alcohols[11] and hydroformylation.[12] It was found that while the electron donating property of the ferrocenyl fragment enhances oxidative addition to the ferrocene-containing *β*-diketonato-rhodium(I) complexes,[10] it has the opposite effect on the rate of substitution of the *β*-diketonato ligand in a series of ferrocene-containing [Rh(*β*-diketonato)(cod)] complexes with 1,10-phenanthroline.[9] Central to the quantification of physical properties and reactivity of ferrocene-containing *β*-diketonato complexes are Gordy scale group electronegativities,[13] χ_R, of the R groups of $(RCOCHCOR')^-$. Thus, χ_R values have been used to approximate $pK'_a = -3.484(\chi_{R'} + \chi_R) + 24.6$,[10] and the formal reduction potentials[14] of the Fc/Fc^+ couple as $E^{\circ\prime}(Fc) = 0.115\ \chi_R - 0.027$ in free neutral *β*-diketones $RCOCH_2COFc$. Group electronegativities were also related to rates of *β*-diketonato substitution[9a] by 1,10-phenanthroline from [Rh(FcCOCHCOR)(cod)] at 25 °C, and to the rate of oxidative addition[10] of methyl iodide to $[Rh(FcCOCHCOR)(CO)(PPh_3)]$. The rhodium oxidation potential,[14,15] as well as the formal reduction potential, $E^{\circ\prime}$, of the ferrocenyl group of these rhodium complexes were shown to be governed by χ_R and the equation[3b] $\nu_{CO} = 5(\chi_{R'} + \chi_R) + 1959$ relates the IR stretching frequencies, ν_{CO}, of $[Rh(RCOCHCOR')(CO)(PPh_3)]$ with group electronegativity.

Octahedral *tris*(*β*-diketonato)aluminum(III) complexes[16] have been studied as organic light emitting diodes,[17] as liquid precursors for chemical vapor deposition,[18] and to understand organic support-metal interactions.[19] They have been synthesized via a variety of routes,[20,21] but the most favored method involves treatment of aluminum sulfate with the *β*-diketone in aqueous ammonia or aqueous ammonia/methanol mixtures. Mixed *β*-diketonato aluminum(III) complexes of the type $[Al(R^1COCHCOR^2)_n(R^3COCHCOR^4)_{3-n}]$[22] and mixed alkoxy *β*-diketonato aluminum(III) complexes of the type $[Al(R^1COCHCOR^2)_n(OR^3)_{3-n}]$[23] are also known. Unsymmetrical *tris*(*β*-diketonato) complexes of aluminum and other metals frequently exhibit *mer*- and *fac*-geometrical isomerism.[24,25] The only known ferrocene-containing *β*-diketonato

Received: August 24, 2011
Published: January 24, 2012

aluminum complex, $[Al(FcCOCHCOCH_3)_3]$, **2**, was reported by Zanello and co-workers.[25] In an electrochemical study in CH_2Cl_2/0.2 M $[N(^nBu)_4][PF_6]$, these authors found no ferrocenyl intramolecular communication whatsoever. This is attributed to the use of $[N(^nBu)_4][PF_6]$ as supporting electrolyte. However, recent advances in voltammetry saw the development of $[N(^nBu)_4][B\{C_6H_3(CF_3)_2\}_4]$ by Mann et al.[26] and also $[N(^nBu)_4][B(C_6F_5)_4]$ by Geiger et al.[27] as supporting electrolytes with a low propensity toward ion pair formation of the type $(\text{cation})^+\cdots{}^-[B(C_6F_5)_4]$. This has allowed Geiger and others[28] to demonstrate electronic communication between differently charged mixed-valent intermediates by means of cyclic voltammetry which was hitherto impossible. It also allowed detection of redox couples involving unstable intermediates that decompose in the presence of $[N(^nBu)_4][PF_6]$ salts, like the Rc/Rc$^+$ couple where Rc = ruthenocene, $Ru^{II}Cp_2$, and Rc$^+$ the unstable d^7 ruthenocenium radical cation, $[Ru^{III}Cp_2]^+$.[27]

In this study we report the synthesis of three new aluminum β-diketonato complexes, $[Al(FcCOCHCOR)_3]$ with R = CF_3, **1**, CH_3, **2**, C_6H_5, **3**, and Fc, **4**, characterize them structurally and highlight intramolecular communication between ferrocenyl groups from results of an electrochemical study in the presence of $[N(^nBu)_4][B(C_6F_5)_4]$. Successive ferrocenyl formal reduction potentials are shown to be a function of χ_R, and the cytotoxicity of $[Al(FcCOCHCOCF_3)_3]$, **1**, against the human cervix epitheloid cancer cell line is discussed.

RESULTS AND DISCUSSION

Synthesis. Complexes **1**–**4** were synthesized by employing several different synthetic procedures, Scheme 1. Treatment of an aqueous solution of aluminum sulfate with 3 equiv of the β-diketone dissolved in methanol and concentrated aqueous ammonia mixtures produced product yields between 26% (for **4**) and 62% (for **2**); see Experimental Section. The acetate anion is often added to reaction mixtures to assist β-diketone complexation to metals.[8] However, in the case of $[Al(FcCOCHCOR)_3]$ formation, addition of sodium acetate to reaction mixtures was counter productive; only **1** gave an isolatable yield (10%). Large quantities of unreacted β-diketone were, however, recovered. This suggests that sodium acetate is not effective at deprotonating the free ferrocene-containing β-diketone ligands. In support of this conclusion, only $FcCOCH_2COCF_3$ (pK_a = 6.53)[8] has a pK_a smaller than the acetate anion pK_b of 7.25. The other β-diketones have pK_a values of 10.01 (R = CH_3), 10.41 (R = Ph), and 13.1 (R = Fc).[8] For the synthesis of $[Al(FcCOCHCOFc)_3]$, **4**, treatment of aluminum trichloride with preformed 1,3-diferrocenylpropane-1,3-dionato lithium(I), $[FcCOCHCOFc]^-Li^+$, Scheme 1 afforded after workup **4** in 25% yield. A ligand exchange reaction where the acetylacetonato ligands in $[Al(H_3CCOCHCOCH_3)_3]$ were exchanged with $FcCOCH_2COFc$ over 48 h while refluxing in acetonitrile gave **4** in only 7% yield probably because the exchange of $H_3CCOCHCOCH_3^-$ with the larger $FcCOCHCOFc^-$ ligand is sterically hindered, and because the pK_a of $FcCOCH_2COFc$ is higher than that of $H_3CCOCH_2COCH_3$ (8.95).[8] Similarly, a beta-diketonato substitution kinetic study on rhodium complexes also showed that leaving ligands having larger pK_a's are slower replaced with incoming ligands than leaving ligands having lower pK_a's.[9]

***mer:fac* Ratios.** Although the symmetrical nature of the ligands of $[Al(FcCOCHCOFc)_3]$ excludes the existence of *mer* and *fac* isomers, the existence of *mer* and *fac* isomers is possible for **1**, **2**, and **3**, Figure 1. It was shown by ^1H NMR spectroscopy that in $CDCl_3$ solutions, **2** and **3** exist as mixtures of three *mer* and one *fac* isomer, but that $[Al(FcCOCHCOCF_3)_3]$ exists only as three *mer* isomers. Figure 2 shows the ^1H NMR spectrum of **3**; that of **1** and **2** is shown in Supporting Information. The methine (COC$\underline{H}$CO) proton resonances of **3** are detected as three signals at 6.46–6.56 ppm exhibiting a ratio of 2:1:1. The three *mer* isomers must generate three methine resonances of equal intensity, while the *fac* isomer can only have one methine resonance because of its symmetrical structure. It follows that a ratio of 3:1 for the *mer*:*fac* content must exist. The *fac* methine signal overlaps with the first of the three *mer* methine signals. Within experimental error, the same *mer*:*fac* ratio is also obtained on analyses of the ferrocenyl signals.

Scheme 1. Synthetic Routes Towards $[Al(FcCOCHCOR)_3]$ Complexes 1–4

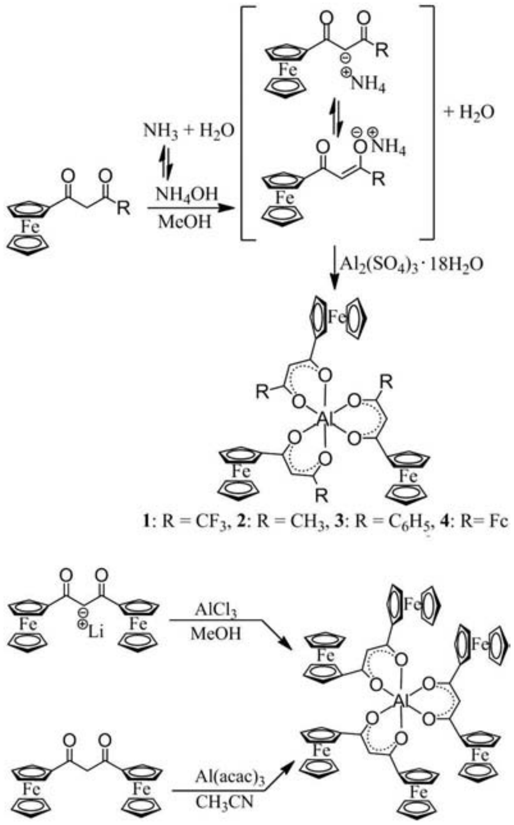

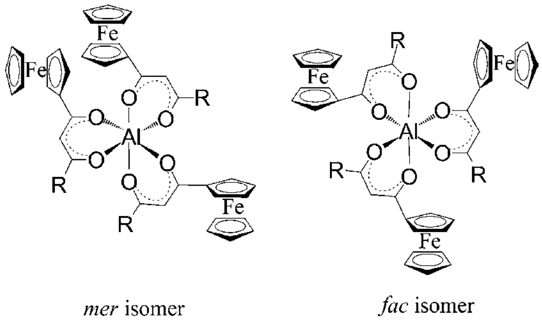

Figure 1. Isomers *mer* and *fac* of **2** (R = CH_3) and **3** (R = Ph). Three different *mer* isomers exist, while the *fac* isomer can only have one methine resonance because of its symmetrical geometry.

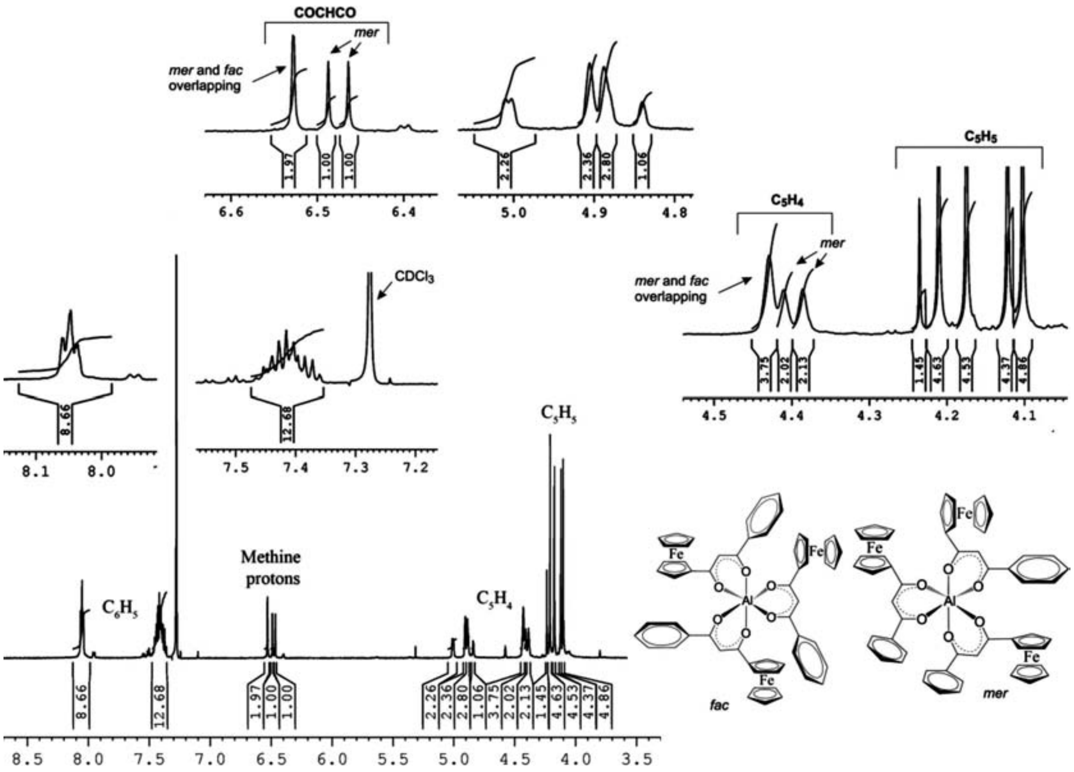

Figure 2. ^{1}H NMR spectrum of [Al(FcCOCHCOPh)$_3$], **3**, in CDCl$_3$. Peak assignments are in the Experimental Section.

Table 1. Crystal Data and Structural Refinement for 1

empirical formula	$C_{42}H_{30}AlF_9Fe_3O_6$	absorption coefficient/mm^{-1}	1.120
molecular weight	996.19	θ range for data collection /deg	1.43 to 28.29
crystal size/mm^3	0.57 × 0.09 × 0.06	index ranges	$-13 \leq h \leq 13$, $-26 \leq k \leq 26$ $-26 \leq l \leq 27$
temperature/K	100(2)	reflections collected	40148
wavelength/Å	0.71073	independent reflections	10516 [R(int) = 0.0642]
crystal system	orthorhombic	completeness to θ = 28.29°	99.9%
space group	$P2_12_12_1$	max. and min transmission	0.9358 and 0.5677
unit cell dimensions /Å	a = 10.3997(9) b = 19.858(2) c = 20.508(2)	refinement method data/restraints/parameters goodness-of-fit on F^2	full-matrix least-squares on F^2 10516/0/551 0.983
volume /Å	4235.2(7)	final R indices [$I > 2\sigma(I)$]	$R1$ = 0.0587, $wR2$ = 0.1384
Z	4	R indices (all data)	$R1$ = 0.0887, $wR2$ = 0.1501
density (calculated) /Mg m^{-3}	1.562	absolute structure parameter	0.035(17)
F(000)	2008	largest diff. peak and hole/e Å^{-3}	1.565 and −0.535

The ratio of *mer*:*fac* methine signals for **2** was found to be 2:1 (see Supporting Information for NMRs), implying a 67% content of *mer* isomers and 33% *fac* isomer content in solution. The ^{1}H NMR of **1** (Supporting Information) only showed the existence of three *mer* methane signals in a ratio of 1:1:1 implying that **1** only exists as the *mer* isomer in CDCl$_3$ solutions.

Single Crystal X-ray Crystallography of 1. To understand the good resolution observed between successive ferrocenyl oxidations described in the next section, an evaluation of the structural characteristics of **1** is informative. [Al(FcCOCHCOCF$_3$)$_3$], **1**, crystallizes from acetone-hexane (1:1) to give an orthorhombic crystal system with $P2_12_12_1$ space group. The refinement parameters and crystal data is shown in Table 1 and different views of the molecular structure of **1**, highlighting atom labeling, are shown in Figure 3. Selected bond distances (Å) and bond angles (deg) are summarized in the caption of Figure 3.

Prior to comparing the three β-diketonato fragment structures of **1**, it is instructive to note that typical C−C single bond lengths range from 1.38 (sp-sp: -C≡**C−C**≡C-) to 1.53 Å (sp^3-sp^3: -**C−C**-), while double bonds range from 1.28 (sp-sp: =**C=C**=) to 1.32 Å (sp^2-sp^2: -**C=C**-).[29] C−C bonds in compounds showing delocalization are expected to have distances that lie between the 1.48 Å of an sp^2-sp^2 =**C−C**= single bond and the 1.32 Å of an sp^2-sp^2 -**C=C**- double bond.[30]

All the C−C bonds in the β-diketonato ligand, except <u>C−CF$_3$</u>, have lengths (l) between 1.32 and 1.48 Å. The shortest bond is C(006)−C(007) (1.342(7) Å, Fe(2) β-diketonato fragment) and the longest is C(51)−C(012) (1.468(7) Å, Fe(3) β-diketonato fragment). Thus, C−C bonds in the β-

diketonato backbone have delocalized character and in principle should be capable of conveying any electron withdrawing and donating effects to and from the ferrocenyl group.

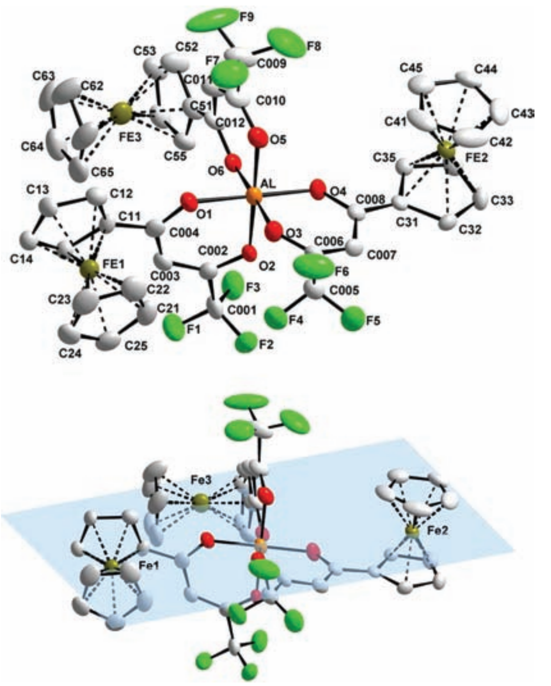

Figure 3. Molecular structure of $[Al(FcCOCHCOCF_3)_3]$, **1**, showing atom labeling (top). The bottom view highlights that the ferrocenyl-fragments of Fe(1) and Fe(2) are perpendicular to the indicated blue plane, while the ferrocenyl-fragment of Fe(3) is parallel to it. Selected bond distances (Å) and angles (deg) [equivalent free $FcCOCH_2COCF_3$ distances in square brackets][6] are: C(11)−C(004) 1.449(7) [1.448(6)], C(003)−C(004) 1.406(7) [1.432(6)], C(002)−C(003) 1.374(7) [1.345(6)], C(001)−C(002) 1.517(7) [1.515(7)], C(004)−O(1) 1.271(6) [1.277(5)], C(012)−O(6) 1.274(6) [1.297(5)], Al−O(1) 1.890(3), Al−O(2) 1.890(3), C(11)−C(12) 1.441(7), C(11)−C(15) 1.423(7); C(002)−C(003)−C(004) 122.1(5) [120.0(4)], O(2)−C(002)−C(003) 128.6(5), O(1)−C(004)−C(003) 121.3(5), O(1)−C(004)−C(11) 118.8(4), O(2)−C(002)−C(001) 111.7(4).

The difference between the two C−C bond lengths around the methine (CH) group in the (O)C−CH−C(O) backbone of the *β*-diketonato ligands identified by Fe(1), Fe(2), and Fe3) are 0.032, 0.104, and 0.054 Å, respectively. Thus, the Fe(2) *β*-diketonato fragment is decisively asymmetric while the Fe(1) and Fe(3) *β*-diketonato fragments are weakly asymmetric. The large difference in electronegativity[6,8] between the ferrocenyl group (χ_{Fc} = 1.87) and the CF_3 group (χ_{CF_3}= 3.01) leads to asymmetric *β*-diketonato ligands showing shorter C−C bonds closer to the CF_3 group in the (O)C−CH−C(O) backbone. The free *β*-diketone, $FcCOCH_2COCF_3$, is also asymmetric, with a difference of C−C-bonds around the CH (methine) group of 0.087 Å. In the free *β*-diketone, enolization occurs away from the ferrocenyl group, implying the smaller (O)C-(CH) bond is closest to the CF_3 group.[6]

Focusing on the ferrocenyl groups, the average C−C bond distance within the ferrocenyl groups is 1.413 Å for the unsubstituted cyclopentadienyl rings and 1.415 Å for substituted cyclopentadienyl rings. The longest bond is C(64)−C(65), 1.445(9) Å, for the unsubstituted cyclopentadienyl ring of the ferrocenyl group containing Fe(3). The shortest bond is C(21)−C(22), 1.359 Å, for the unsubstituted cyclopentadienyl ring of the ferrocenyl group containing Fe(1). Delocalized bonding thus occurs within each of the separate ferrocenyl groups and electron withdrawing or donating effects from electrochemically generated charged ferrocenium (Fe^{3+}) and neutral ferrocenyl (Fe^{2+}) centers may be transmitted through the *β*-diketonato backbones to each other.

All three ferrocenyl groups were found to exist almost exactly in the eclipsed form. The deviation from eclipsed form, as measured with the dihedral angles C(21)-centroid$_{Cp\ ring}$-centroid$_{subst\ Cp\ ring}$-C(11), C(41)-centroid$_{Cp\ ring}$-centroid$_{subst\ Cp\ ring}$-C(31) and C(61)-centroid$_{Cp\ ring}$-centroid$_{subst\ Cp\ ring}$-C(51), were 1.405(8)°, 4.355(8)°, and 0.890(8)°, respectively. Bond angles in both the unsubstituted and the substituted cyclopentadienyl rings averaged 108°, the ideal theoretical value. The largest deviations from the average values were C(25)−C(21)−C(22) (+2.5°) on a substituted C_p ring and C(12)−C(13)−C(14) (+2.0°) on an unsubstituted C_p ring, both occurring in the cyclopentadienyl rings centered on Fe(1).

Typical unconjugated C═O bond lengths in *β*-diketones are 1.206 Å, while C−O bond lengths are 1.300 Å.[31] For **1**, all the C−O bonds lengths are between these extremes. The shortest is C(004)−O(1) with a length of 1.271(6) Å and the longest is C(010)−O(5) = 1.289(6) Å). The difference between the longest and shortest C−O bonds is 0.018 Å, while the difference between unconjugated C═O and C−O bonds in *β*-diketones is 0.094 Å. It is clear that the C−O bonds encountered in **1** are much longer than typical C═O bonds and meaningfully shorter than C−O bonds and are thus also indicative of significant delocalized character in all three *β*-diketonato fragments. Because of all the conjugated bonds in the *β*-diketonato ligands, each ligand should in principle be capable of transmitting through-bond electronic communication from one end of the ligand to the other. The remaining question to be answered to understand if one *β*-diketonato ligand of **1** can transmit any electronic effects it may have to another is an understanding of how these effects may cross the aluminum core of these complexes.

The aluminum atom in $[Al(FcCOCHCOCF_3)_3]$, **1**, has an octahedral coordination sphere. The average Al−O bond length is 1.881 Å. The largest deviations from this average is 0.024 Å for Al−O(6) which has a bond length of 1.905(3). Al−O(5) has a bond length of 1.859(4) Å. Al−O(1) and Al−O(2) have equal bond lengths of 1.890(3) Å and so do Al−O(3) and Al−O(4) (1.868(3) Å). A crystal packing effect is the most probable reason for the inequality of Al−O(5) and Al−O(6) bond lengths. The difference between the largest (Al−O(6)) and smallest (Al−O(5)) Al−O bond lengths is 0.046 Å. The close agreement of all the Al−O bond lengths suggests that good through-bond electronic communication will be possible through the Al core of **1**. The capability of **1** to transmit electronic effects from one end of the molecule to the other was studied and quantified with the mathematical formulas in the electrochemical section of this study.

The average O−Al−O bond angle is 91.28° with the largest deviation from the average being 0.59° for O(5)−Al−O(6). These values are in close agreement with literature values.[23,24] $Al(acac)_3$ has Al−O bonding distances ranging between 1.871 Å for the *δ*-polymorph to 1.890 Å for the *γ*-polymorph and the O−Al−O bonding angles range from 90.19° to 90.81°.

Thus, summarizing, the crystal structure of **1** suggests good electronic communication between the different ferrocenyl moieties is possible because of the delocalized nature of the C—C backbone in the *β*-diketonato fragments and the almost equivalent C—O and Al—O bonds.

Electrochemistry. Cyclic voltammetry (CV), linear sweep voltammetry (LSV), and square-wave voltammetry (SW) were conducted on **1**−**4** in dry CH_2Cl_2 utilizing 0.1 mol dm^{-3} $[N(^nBu)_4][B(C_6F_5)_4]$ as supporting electrolyte to minimize any solvent-compound interactions.[27] Data for cyclic voltammetry experiments are summarized in Table 2. All potentials are referenced against Fc/Fc^+ as suggested by IUPAC;[32] however, decamethylferrocene (Fc*) was used as internal reference to avoid overlap of the signals of the ferrocenyl groups in each complex with the signal of free ferrocene.[33] Under our experimental conditions the $(Fc^*)/(Fc^*)^+$ couple was found to be at −609 mV versus Fc/Fc^+. The only metallic redox active centers in the compounds series **1**−**4** are the iron centers of the ferrocenyl groups.

Table 2. Cyclic Voltammetry Data[a] of 0.5 mmol dm^{-3} Solutions of Analytes in Dry CH_2Cl_2 Containing 0.1 mol dm^{-3} $[N(^nBu)_4][B(C_6F_5)_4]$ as Supporting Electrolyte at 25 °C

wave	E_{pa}/V	ΔE_p/mV	$E^{o\prime}$/V	i_{pa}/μA	i_{pc}/i_{pa}
Decamethylferrocene (Fc*)					
-	−575	68	−609	3.24	0.95
$Al(FcCOCHCOCF_3)_3$, **1**					
1	313	66	280	3.1	1.11
2	439	72	403	3.2	1.05
3	569	72	533	3.2	0.90
$Al(FcCOCHCOCH_3)_3$, **2**					
1	117	62	86	3.53	1.04
2	235	66	202	3.53	0.92
3	325	64	293	3.52	0.92
$Al(FcCOCHCOPh_3)_3$, **3**					
1	131	62	100	1.94	1.17
2	241	68	207	1.94	1.00
3	331	66	298	1.94	1.13
$Al(FcCOCHCOFc)_3$,**4**					
1	64	62	33	0.36	0.33[b]
2	154	62	123	0.39	1.08
3	340	72[b]	304	0.45	1.07
4	460	56	432	0.42	0.86
5	614	62	583	*b*	*b*
6	770	58	741	*b*	*b*

[a] Potentials versus Fc/Fc^+, scan rate =100 mV s^{-1}. [b] Because of the large overlap of peaks and poor peak resolution, the indicated currents and i_{pc}/i_{pa} ratios could either not be obtained or they differ substantially from unity. For the same reason, the indicated ΔE_p values deviate slightly from the other values in the table. It should be recognized that the above data represent "observed" potentials and current ratios rather than theoretically simulated values. They could not be simulated with confidence because of too many unknowns, including the diffusion constants of electrochemically generated intermediates.

The CVs of **1**−**3** shown in Figure 4 each displayed three ferrocene-related oxidation half reactions in the anodic CV sweep (the peaks pointing upward) and reduction half reactions in the cathodic CV sweep (the peaks pointing downward). Each of the three ferrocenyl substituents showed reversible electrochemical behavior at slow scan rates with $\Delta E_p < 70$ mV.

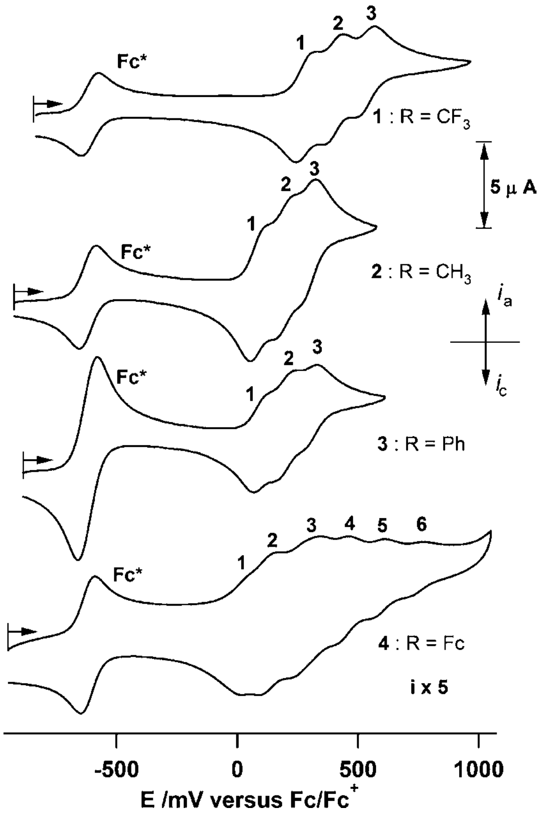

Figure 4. Cyclic voltammograms of about 0.5 mmol dm^{-3} solutions of $Al(FcCOCHCOR)_3$ **1**−**4** at 100 mV s^{-1} in CH_2Cl_2/0.1 mol dm^{-3} $[NBu_4][B(C_6F_5)_4]$ at 25 °C. Because of the lower solubility (ca. 0.1 mmol dm^{-3}) of $Al(FcCOCHCOFc)_3$, its current signal is scaled by a factor of 5.

Theoretically, electrochemical reversibility is characterized by ΔE_p values of 59 mV.[34,35] However, at higher scan rates (500 mV s^{-1}, see Supporting Information) the differences in peak potentials increased to almost 90 mV. LSV confirmed three separate one-electron transfer processes for the oxidation of the three ferrocene substituents.

Although **4** exhibited low solubility in dichloromethane, a sufficient quantity could be dissolved in dichloromethane to perform an electrochemical analysis. CVs, LSVs, and SWs of $Al(FcCOCHCOFc)_3$, **4**, are shown in Figure 5. All six ferrocene oxidations and reductions are observed and could be resolved; peaks are labeled as 1 through 6. Although the first oxidation, wave 1, appears as a shoulder on the CV of **4**, Osteryoung square wave voltammetry afforded enough extra resolution to clearly show that the electrochemistry of all six ferrocene substituents can be resolved. The LSV confirmed all six electron transfer processes involve the flow of only one electron. The electrochemical processes are summarized in Scheme 2. The low effective concentration of dissolved **4** in the solvent most likely contributed to the high peak resolution obtained during the experiments.

From Figure 4 and Table 2 it is clear that $E^{o\prime}$ values for complexes **1**−**4** span over a huge potential range, from 33 to 741 mV. This striking result is only possible if the electron density of the iron centers in each complex is effectively influenced by the electron withdrawing or electron donating properties of other Fc or Fc^+ groups in neutral and oxidized derivatives of **1**−**4**. All other molecular fragments of the complexes remain unchanged during the course of the

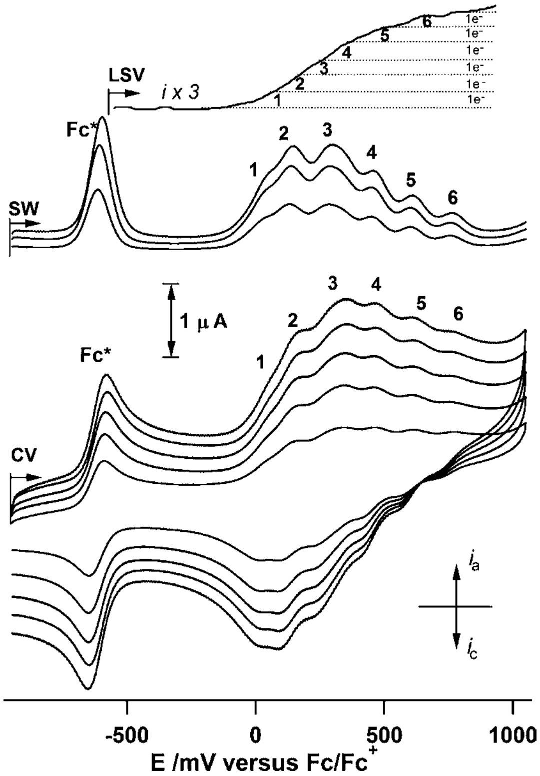

Figure 5. Linear sweep (top), Osteryoung square wave (middle) and cyclic voltammograms (bottom) of **4** in CH_2Cl_2/0.1 mol dm^{-3} [$N(^nBu)_4$][$B(C_6F_5)_4$] on a glassy carbon-working electrode at scan rates of 100, 200, 300, 400, and 500 mV/s for cyclic voltammograms and 1 mV/s for LSV. Osteryoung square wave voltammetry was performed at 5, 10, and 15 Hz. Decamethylferrocene, Fc*, was used as internal standard. Fc* has a potential of −609 mV versus Fc/Fc$^+$. Arrows show the onset potential and scan direction. The current of the LSV experiment was scaled by a factor of 3 to afford better interpretation.

Scheme 2. Electrochemical Processes Associated with Waves 1−6 of Al(FcCOCHCOFc)$_3$, 4^a

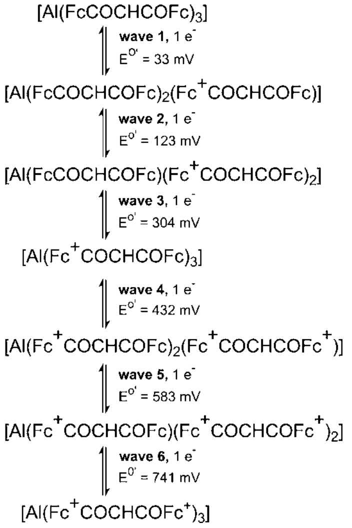

[a]$E^{0\prime}$ values are given at a scan rate of 100 mV s^{-1}.

electrochemistry experiments and are therefore not the cause for the observed different CV peak potentials. To explain and quantify the observed different potentials, use was made of the group electronegativities of the different R groups. The group electronegativity, χ_R, for each R group[6,8] is χ_{Fc} = 1.87, χ_{CH3} = 2.34, χ_{Ph} = 2.21, χ_{Fc+} = 2.82, and χ_{CF_3} = 3.01. It was previously shown that $E^{\circ\prime}$ can be expressed linearly as a function of the sum of group electronegativities in complexes of the type [Rh(FcCOCHCOR)(CO)$_2$][36] and also as the sum of the group electronegativities of mesosubstituents, $\chi_{R^1} + \chi_{R^2} + \chi_{R^3} + \chi_{R^4}$, for porphyrins.[37]

This approach was applied to complexes **1−4**, first on each complex individually and second, for all complexes unified in one relationship. Here the sum of the group electronegativities is always from six components in the *tris*-ligated complexes Al(FcCOCHCOR)$_3$, that is, from three ferrocenyl and three R-groups. To explain the approach that was used, consider peak 2 of Al(FcCOCHCOCH$_3$)$_3$ (**2**). Peak 2 represents the couple:

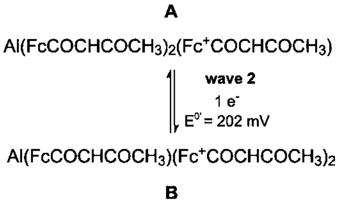

If the reduced and oxidized forms of the couple are labeled A and B, respectively, then for A

$$\begin{aligned}\sum \chi_R &= 2(\chi_{Fc} + \chi_{CH_3}) + (\chi_{Fc^+} + \chi_{CH_3})\\ &= 2(1.87 + 2.34) + (2.82 + 2.34)\\ &= 13.58\end{aligned}$$

Thus, a measure of the electron density on **2**$^+$ (from A of **2** above) that is to be oxidized at wave 2 is $\sum\chi_R$ = 13.58. The sum of electron density associated with the ferrocenyl group being oxidized was calculated for all electron transfer processes of all the compounds in a similar manner. Figure 6 (left) shows this relationship for each compound separately.

For each complex separately, a linear relationship between $E^{\circ\prime}$ and $\sum\chi_R$ was observed. The equations predicting $E^{\circ\prime}$ from $\sum\chi_R$ for **1−4** were found to be as follows:

$$\text{for } \mathbf{1}\text{:} \quad E^{\circ\prime} = 133.1 \sum \chi_R - 1670 \tag{1}$$

$$\text{for } \mathbf{2}\text{:} \quad E^{\circ\prime} = 108.9 \sum \chi_R - 1285 \tag{2}$$

$$\text{for } \mathbf{3}\text{:} \quad E^{\circ\prime} = 104.2 \sum \chi_R - 1172 \tag{3}$$

$$\text{for } \mathbf{4}\text{:} \quad E^{\circ\prime} = 151.8 \sum \chi_R - 1694 \tag{4}$$

In an attempt to unify the relationship between $E^{\circ\prime}$ and $\sum\chi_R$ for all observed electrochemical processes of **1−4**, Figure 6 (right) was constructed. Peaks 3, 4, 5, and 6 of [Al(FcCOCHCOFc)$_3$], **4**, were not used to fit the combined relationship in Figure 6 because they clearly did not fit the trend set by all other ferrocene related electrochemical processes of complexes **1−4**. This may be a consequence of the large number of positive charges in close proximity that is generated when **4** is oxidized for the third to the sixth time. The resulting "sea" of cations may induce electrostatic effects that contribute to this deviation. The data predicts a near linear relationship between $E^{\circ\prime}$ and $\sum\chi_R$ with the possible exception of the two extreme data points, Fc-1 and CF$_3$-3. The least-

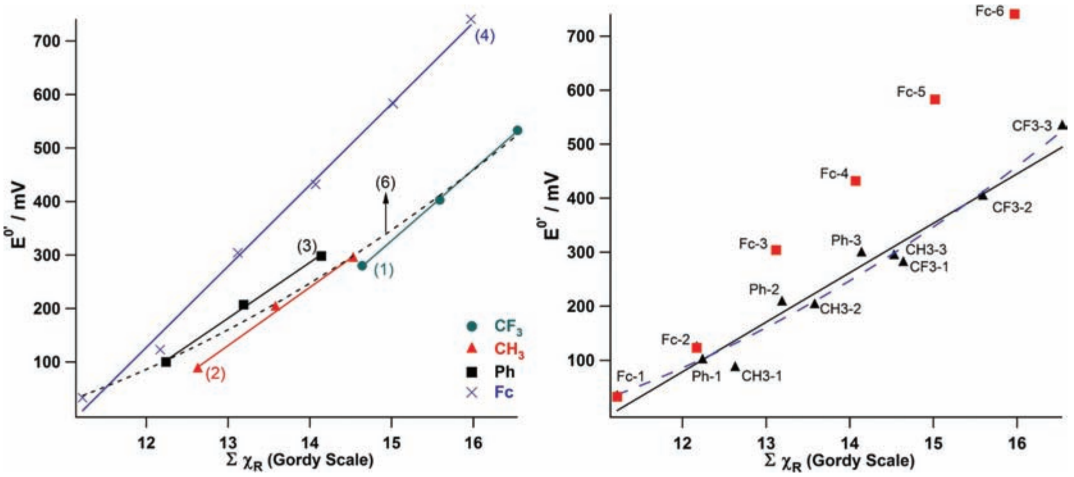

Figure 6. Relationship between the sum of the group electronegativities and the redox potentials, for each compound individually (left), and for all the compounds combined (right). The number following each substituent indicates which ferrocene/ferrocenium couple is referred to. Example: CF3−2 indicate the $E^{\circ\prime}$ value of the second ferrocenyl group being oxidized in the complex $\mathrm{Al(FcCOCHCOCF_3)_3}$.

squares linear fit gave eq 5 with $R^2 = 0.960$ (the black solid line in Figure 6, right), while a quadratic least-squares fit of the data gave eq 6 with $R^2 = 0.972$ (the blue broken line in Figure 6, right),

$$E^{\circ\prime} = 91.52 \sum \chi_R - 1019 \quad (5)$$

$$E^{\circ\prime} = 6.313\left(\sum \chi_R\right)^2 - 83.53 \sum \chi_R - 179.2 \quad (6)$$

Cytotoxicity of 1. The cytotoxicity of ferrocene-containing complexes are frequently dependent on the formal reduction potential of the ferrocenyl group. For example, for ferrocene alcohols, it was found that smaller $E^{\circ\prime}$ values lead to higher cytotoxicity (or lower $\mathrm{IC_{50}}$ values; the lowest $\mathrm{IC_{50}}$ value correspond to the more active compound.)[38] In contrast, the free *β*-diketones $\mathrm{FcCOCH_2COR}$ which were the ligands in **1**−**5** followed exactly the opposite trend.[5b]

Two mechanisms by which the ferrocenyl group destroys antineoplastic growths were identified. In the first, the ferrocenyl group reduces the tyrosyl radical of the R2 subunit of the enzyme ribonucleotide reductase.[39] The active site of dimeric R2 consists of a tyrosyl radical and two Fe(III) centers which are *μ*-oxo bridged. Ribonucleotide reductase catalyzes the reduction of ribonucleotides to deoxyribonucleotides, a key step in DNA syntheses, and it is therefore also a target in chemotherapy.[40] The second mechanism was shown to involve an electron transfer process[41] between an oxidized ferrocenium group and water. One of the reaction products is hydroxy radicals which cleaves DNA strands. This mechanism requires a ferrocene-containing drug that must, after it is administered to the body, first be oxidized by redox-active body enzymes to the ferrocenium species to show antineoplastic activity. Indications are that the cutoff formal reduction potential of the ferrocenyl group where this cannot happen any more is 0.02 V vs Fc/$\mathrm{Fc^+}$.[5a,38] The *β*-diketonato ligands of **1**−**4** though operate by a different mechanism because the free ligands $\mathrm{FcCOCH_2COR}$ with $E^{\circ\prime} = 0.187$−317 V vs $\mathrm{Fc/Fc^+}$ are very cytotoxic.[5b] Only the second and third $E^{\circ\prime}$ of the ferrocenyl group of **1** and the fourth, fifth, and sixth $E^{\circ\prime}$ of **4** are larger than 0.317 V, Table 1, implying **1**−**4** may all exhibit cytotoxic activity.

To determine if compounds of the type $\mathrm{Al(FcCOCHCOR)_3}$ may have antineoplastic properties, the cytotoxicity of **1** was determined against the HeLa (human cervix epitheloid) cell line. A cell survival curve as a function of concentration of **1** is shown in Figure 7.

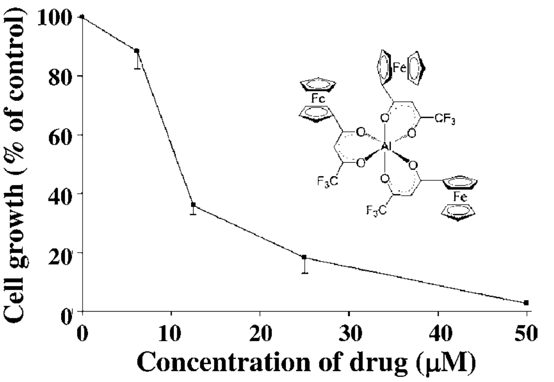

Figure 7. Effect of concentration of $[\mathrm{Al(FcCOCHCOCF_3)_3}]$, **1**, on the survival of human HeLa cancer cells after 7 days of incubation measured as a percentage of untreated controls. Data are presented as mean drug concentration ± standard error of the mean of four experiments.

The mean drug concentration of **1** from 4 experiments causing 50% cell growth inhibition, the $\mathrm{IC_{50}}$ value, was 10.6 ± 0.6 *μ*mol $\mathrm{dm^{-3}}$. Complex **1** was about 50 times less cytotoxic than cisplatin ($\mathrm{Pt(NH)_3Cl_2}$, which has $\mathrm{IC_{50}} = 0.19 \pm 0.1$ *μ*mol $\mathrm{dm^{-3}}$ under identical conditions.[42] The $\mathrm{IC_{50}}$ of free $\mathrm{FcCOCH_2COCF_3}$ is 6.8 *μ*mol $\mathrm{dm^{-3}}$).[5b] If one bears in mind that **1** has three $\mathrm{(FcCOCHCOCF_3)^-}$ ligands, and on the assumption that the $\mathrm{Al^{3+}}$ core does not contribute to **1**'s antineoplastic activity, it follows that **1** is almost (10.6 × 3)/6.8 ≈ 5 times less cytotoxic than the neutral free ligand, $\mathrm{FcCOCH_2COCF_3}$. These results show that the $\mathrm{Al^{3+}}$ core, unlike the Rh(cod) core in [Rh(FcCOCHCOPh)(cod)],[14] does not lead to any positive antineoplastic synergistic effects. Rather, it acts as an inhibiter of the HeLa antineoplastic activity of $\mathrm{FcCOCH_2COCF_3}$.

■ CONCLUSIONS

$\mathrm{Al(FcCOCHCOR)_3}$ complexes with substituents R spanning a range of group electronegativities from 1.87 (Fc), 2.21 (Ph), and 2.34 (CH_3) to 3.01 (CF_3) were synthesized. ^1H NMR studies indicated that the CH_3 and Ph complexes exist as a mixture of three *mer* and one *fac*-isomers in $CDCl_3$. In contrast, no evidence could be found for the existence of a *fac*-isomer of $Al(FcCOCHCOCF_3)_3$. The structure of one of the three *mer*-isomers of the CF_3 complex was solved by single crystal X-ray crystallography. That good communication between pendent *β*-diketonato substituents exists was proved and quantified by an electrochemical study. All the Fc/Fc^+ couples of **1**−**4** were resolved with formal reduction potentials in the range $33 < E^{\circ\prime} < 741$ mV. For each complex, a unique linear relationship exists between the formal reduction of the Fc/Fc^+ couples of each complex and the sum of the group electronegativities, $\sum\chi_R$, of the six pendent *β*-diketonato end groups (two on each $FcCOCHCOR^-$ ligand). Barring the last four oxidations of $[Al(FcCOCHCOFc)_3]$, these could be unified in a linear relationship from which $E^{\circ\prime}$ of the remaining 11 ferrocene-related redox processes could be approximated by the equation, $E^{\circ\prime} = 91.52\sum\chi_R - 1019$. Complex **1** having IC_{50} = 10.6 μmol dm^{-3} is less cytotoxic than the free, neutral $FcCOCH_2COCF_3$ ligand (IC_{50} = 6.8 μmol dm^{-3}), and approximately 2 orders of magnitude less cytotoxic to human HeLa neoplastic cells than cisplatin (IC_{50} = 0.19 μmol dm^{-3} under similar conditions). Results are consistent with the Al^{3+} core acting as an inhibiter of the antineoplastic properties of the *β*-diketonato ligands, $FcCOCH_2COR$.

■ EXPERIMENTAL SECTION

General Information. Solid reagents ($Al_2(SO_4)_3$ and $Al(acac)_3$; Aldrich) were used without any further purification. Organic solvents were dried and or distilled directly prior to use where specified. Doubly distilled water was used. Column chromatography was performed on Kieselgel 60 (Merck, grain size 0.040−0.063 nm) using hexane:diethyl ether (1:1) as mobile phase unless otherwise specified. The free ligands $FcCOCH_2COR$, with R = CF_3, CH_3, Ph, and Fc were synthesized as described before.[6] The salt Li-[FcCOCHCOFc] was isolated from the synthesis of $FcCOCH_2COFc$ by diethyl ether precipitation and filtration prior to washing with copious amounts of diethyl ether. The electrolyte $[N(^nBu)_4][B(C_6F_5)_4]$ was synthesized utilizing the procedure as described by Geiger.[43] ^1H NMR spectra at 20 °C were recorded on a Bruker Advance DPX 300 NMR spectrometer at 300 MHz with chemical shifts presented as δ values referenced to $SiMe_4$ at 0.00 ppm utilizing $CDCl_3$ as solvent. The $CDCl_3$ was made acid free by passing it through basic alumina immediately before use. Cytotoxicity tests were performed as described before[5b,42] utilizing the HeLa cell line from the ATCC CCL-2, American Type Culture Collection, Manassas, Virginia, U.S.A. Cell survival was measured by means of the colorimetric 3-(4,5-dimethylthiazol-2-yl)-diphenyltetrazolium bromide (MTT).

Aluminum Complex Synthesis. *Aqueous Ammonia/Methanol Method.* The synthesis of **3** may serve as an example.

Tri-(1-ferrocenyl-3-phenyl-1,3-dionato-κ²-O,O′) aluminum(III), ***3***. A stirred solution of 1-ferrocenyl-2-phenylpropane-1,3-dione (122 mg, 0.368 mmol) and concentrated (25%) aqueous ammonia (5 cm^3) in methanol (20 cm^3) was added dropwise to a solution of aluminum sulfate octadecahydrate (82 mg, 0.123 mmol) in water (2 cm^3). After stirring for 4 h, a red precipitate was filtered off and washed with water (3 × 30 cm^3). The precipitate was then dissolved in a minimum volume of dichloromethane, and the resulting solution washed with water (3 × 30 cm^3). The organic layer was dried over anhydrous $MgSO_4$ and evaporated. Chromatography of the residue using hexane:diethyl ether (1:1) (R_f = 0.4) as eluent produced 35 mg (50%) of a mixture of *mer* (75%) and *fac*-isomers (25%). There are three *mer* isomers, each of which are present at about 25% of the total constent of **3**. Melting point = 207 °C; ^1H NMR δ_H (300 MHz, $CDCl_3$)/ppm: *fac*-isomer (3 *β*-diketonato ligands per *fac* isomer): 4.21 (m; 3 × 5H; 3 × C_5H_5); 4.43 (m; 3 × 2H; fraction of 3 × C_5H_4 − signal overlaps with 3 × C_5H_4 2H signals of one *mer* isomer); 5.1 (m; 3 × 2H; fraction of 3 × C_5H_4); 6.53 (s; 3 × 1H; 3 × CH); 7.36−7.46 (m; 3 × 3H, fraction of 3 × C_6H_5 signals overlapping with signals of *mer* isomer); 8.05 (m, 3 × 2H, fraction of 3 × C_6H_5 signals overlapping with signals of *mer* isomer); *mer*-isomers (three isomers, each with three *β*-diketonato ligands): 4.10 (s; 3 × 5H; 3 × C_5H_5); 4.12 (s; 3 × 5H; 3 × C_5H_5); 4.17 (s; 3 × 5H; 3 × C_5H_5); 4.38 (m; 3 × 2H; fraction of 3 × C_5H_4); 4.41 (m; 3 × 2H; fraction of 3 × C_5H_4); 4.43 (m; 3 × 2H; fraction of 3 × C_5H_4 − signal overlaps with 3 × C_5H_4 2H signals of the *fac* isomer); 4.84 (m; 3 × 1H; fraction of 3 × C_5H_4); 4.88 (m; 3 × 3H; fraction of 3 × C_5H_4); 4.91 (m; 3 × 2H; fraction of 3 × C_5H_4); 6.46 (s; 3 × 1H; 3 × CH); 6.49 (s; 3 × 1H; 3 × CH); 6.53 (s; 3 × 1H; 3 × CH); 7.36−7.46 (m; 3 × 3H, fraction of 3 × C_6H_5 signals overlapping with signals of *fac* isomer); 8.05 (m, 6H, fraction of C_6H_5 signals overlapping with signals of *fac* isomer). Calculated for $C_{57}H_{45}AlFe_3O_6$: C, 67.09; H, 4.44; Found: C, 66.67; H, 4.52.

Characterization Data of ***1***. The resulting precipitate from aqueous ammonia/methanol synthesis was dissolved in a minimum of dichloromethane (ca. 30 cm^3). The organic solution was washed with water (3 × 30 cm^3), dried ($MgSO_4$), evaporated, and the residue chromatographed with acetone:petroleum ether (1.5:8.5, R_f = 0.43) to give 0.028 g (32%). This compound exists as three *mer*-isomers each having three *β*-diketonato ligands only: no *fac* isomer was observed, mp = 187 °C. ^1H NMR, δ_H (300 MHz, $CDCl_3$)/ppm: 4.18 (s; 3 × 5H; 3 × C_5H_5); 4.30 (s; 6 × 10H; 6 × C_5H_5 − signals of two isomers were overlapping); 4.65 (m; 3 × 7H; fraction of 9 × C_5H_4); 4.92 (m; 3 × 5H; fraction of 9 × C_5H_4); 6.10 (s; 3 × 1H; 3 × CH); 6.14 (s; 3 × 1H; 3 × CH); 6.15 (s; 3 × 1H; 3 × CH). Calculated for $C_{42}H_{30}AlFe_3F_9O_6$: C, 50.64; H, 3.04; Found: C, 50.30; H, 3.22.

Characterization Data of ***2***. Evaporation of the dichloromethane layer gave a precipitate that was washed with acetone (3 × 10 cm^3) and air-dried to give 0.063 g (62%) of pure **2** that existed as a mixture of three *mer* isomers (62% in total, i.e., about 21% for each *mer* isomer) and one *fac* isomers (38%). Mp 250 (dec.). ^1H NMR δ_H (300 MHz, $CDCl_3$)/ppm: *fac*-isomer (three *β*-diketonato ligands): 2.10 (s; 3 × 3H; 3 × CH_3); 4.23 (m; 3 × 5H; 3 × C_5H_5); 4.41 (m; 3 × 2H; fraction of 3 × C_5H_4 - signal overlaps with 6 × C_5H_4 2H signals of the *mer* isomer); 4.76 (m; 3 × 2H; fraction of 3 × C_5H_4); 5.77 (s; 3 × 1H; 3 × CH); *mer*-isomers (three isomers, each with three *β*-diketonato ligands): 2.11 (s; 3 × 3H; 3 × CH_3); 2.12 (s; 3 × 3H; 3 × CH_3); 2.17 (s; 3 × 3H; 3 × CH_3); 4.12 (s; 3 × 5H; 3 × C_5H_5); 4.22 (s; 3 × 5H; 3 × C_5H_5); 4.26 (s; 3 × 5H; 3 × C_5H_5); 4.35 (m; 3 × 2H; fraction of 3 × C_5H_4); 4.38 (m; 3 × 4H; fraction of 6 × C_5H_4 - signal overlaps with 3 × C_5H_4 2H signals of the *fac* isomer); 4.79 (m; 3 × 2H; fraction of 3 × C_5H_4); 4.85 (m; 3 × 1H; fraction of 3 × C_5H_4); 4.87 (m; 3 × 1H; fraction of 3 × C_5H_4); 4.91 (m; 3 × 2H; fraction of 3 × C_5H_4); 5.74 (s; 3 × 1H; 3 × CH); 5.77 (s; 3 × 1H; 3 × CH); 5.81 (s; 3 × 1H; 3 × CH). Calculated for $C_{42}H_{39}AlFe_3O_6$: C, 60.47; H, 4.71; Found: C, 60.24; H, 4.58.

tris(1,3-Diferrocenylpropane-1,3-dionato-κ²-O,O′) Aluminum(III), ***4***. *Method A:* The aqueous ammonia/methanol method gave 26% of pure **4** after workup.

Method B: The reaction *between Li[FcCOCHCOFc] and* Al^{3+}. A solution of 1,3-diferrocenylpropane-1,3-dionato lithium(I) (100 mg, 0.224 mmol) in methanol (10 cm^3) was added dropwise to a solution of $AlCl_3$ (10 mg, 0.075 mmol) in water (1 cm^3). An orange-colored precipitate was filtered off and washed with water (3 × 10 cm^3) and acetone (3 × 10 cm^3) and dried in air to give 25 mg (23%) clean **4**.

Method C: Ligand exchange of $Al(acac)_3$. A solution of aluminum *tris*-acetylacetonate (12.3 mg, 0.038 mmol) and 1,3-diferrocenylpropane-1,3-dione (50 mg, 0.114 mmol) in acetonitrile (15 cm^3) was refluxed for 3 h. The solvent was then reduced to ±2 cm^3 and an orange precipitate filtered off and washed with ether (3 × 10 cm^3) to give 10.2 mg (7%) clean product, mp >250 °C. Complex **4** was too insoluble in readily available NMR solvents for measurements, but electrochemical and elemental analyses confirmed the product to be **4**. Calculated for $C_{69}H_{57}AlO_6Fe_6$: C, 61.60; H, 4.35; Al, 2.01; Fe, 24.93 O, 7.14; Found: C, 61.34; H, 4.72; Al, 1.83; Fe, 24.59 O, 6.63.

*Crystal Structure Determination of **1**.* A red plate-like crystal of **1** with approximate dimensions 0.575 × 0.094 × 0.06 mm^3 was mounted on a glass fiber and used for the X-ray crystallographic analysis. The X-ray intensity data were measured on a Bruker X8 Apex II 4K CCD area detector diffractometer equipped with a graphite monochromator and Mo−Kα fine-focus sealed tube (λ = 0.71073 Å) operated at 1.5 KW power (50 KV, 30 mA). The detector was placed at a distance of 3.75 cm from the crystal. Crystal temperature during the data collection was kept constant at 100(2) K using an Oxford 700 series cryostream cooler.

The initial unit cell and data collection were achieved by Apex2 software[44] utilizing COSMO[45] for optimum collection of more than a hemisphere of reciprocal space. A total of 862 frames were collected with a scan width of 0.5 in φ and ω, and an exposure time of 250 s $frame^{-1}$. The frames were integrated using a narrow frame integration algorithm and reduced with the Bruker SAINTPlus and XPREP[46] software packages respectively. Analysis of the data showed no significant decay during the data collection. Data were corrected for absorption effects using the multiscan technique SADABS.[47] The structure was solved by the direct methods package SIR97[48] and refined using the WinGX[49] software package incorporating SHELXL.[50] The aromatic protons were placed in geometrically idealized positions (C−H = 0.95 Å) and constrained to ride on their parent atoms with $U_{iso}(H) = 1.2U_{eq}(C)$. Non-hydrogen atoms were refined with anisotropic displacement parameters. Atomic scattering factors were taken from the International Tables for Crystallography Volume C. The molecular plot was drawn using the DIAMOND[51] program with a 50% thermal envelope probability for non-hydrogen atoms. Hydrogen atoms were drawn as arbitrary sized spheres with a radius of 0.135 Å. Several attempts to refine a satisfactory solvent model in the lattice failed, and in the final refinement of the data it was treated with the SQUEEZE[52] procedure to remove reflections contributing to the area of the solvent.

Electrochemical Study. Cyclic voltammetry, square wave voltammetry, and linear sweep voltammetry were conducted on a BAS 100 B/W voltammograph utilizing a three-electrode configuration. Potentials were referenced experimentally to a Vicor-tipped, in-house constructed Ag/AgCl reference electrode immersed in an acetonitrile Luggin capillary bridged by a second capillary containing CH_2Cl_2. The AgCl-coated silver wire was prepared by anodic electrolysis of the wire in a 1 M HCl solution using a potential of 1.5 V and a 20 μA current for a period of 30 s. It should be noted this electrode resulted in large potential drifts during successive voltammetric measurements. Hence each experiment had to be conducted in the presence of an internal standard, here decamethyl ferrocene, to allow manual correction of data on a spread sheet program. A glassy carbon working electrode and Pt auxiliary electrode was used.

Analyte concentrations were about 0.5 mM in spectrochemical grade CH_2Cl_2 (Aldrich) and 0.1 M tetrakispentafluorophenylborate, $[N(^nBu)_4][B(C_6F_5)_4]$ were used as solvent/supporting electrolyte. The supporting electrolyte was also present within the acetonitrile and CH_2Cl_2 Luggin capillary. Analyses were performed at 20 °C temperatures and under nitrogen. Decamethylferrocene (Fc*) was used as an internal standard but all potential values are reported against ferrocene at 0 mV. Decamethylferrocene has a potential of −609 mV versus free ferrocene under our conditions. Data were exported to a spread sheet program for manipulation and diagram preparation.

ASSOCIATED CONTENT

Supporting Information

NMR spectra of **1** and **2**, a table giving additional electrochemical data at different scan rates, and the cif file and other crystallographic material of **1**. This material is available free of charge via the Internet at http://pubs.acs.org.

AUTHOR INFORMATION

Corresponding Author

*E-mail: swartsjc@ufs.ac.za.

Present Address

†Department of Chemistry, University of Johannesburg, P.O. Box 524, Auckland Park, 2006, Republic of South Africa.

ACKNOWLEDGMENTS

The authors acknowledge the UFS and SASOL for financial support.

REFERENCES

(1) Spanig, F.; Kolvacs, C.; Hauke, F.; Ohlubo, K.; Fukuzumi, F.; Guldi, D. M.; Hirsch, A. *J. Am. Chem. Soc.* **2009**, *131*, 8180.

(2) (a) Klapars, A.; Clampos, K. R.; Chen, C.; Volante, R. P. *Org. Lett.* **2005**, *7*, 1185. (b) Shen, Q.; Shekhar, S.; Stambuli, J. P.; Hartwig, J. F. *Angew. Chem., Int. Ed.* **2005**, *44*, 1371. (c) Percec, V.; Bae, L.-Y.; Hill, D. H. *J. Org. Chem.* **1995**, *60*, 1060.

(3) (a) Lamprecht, G. J.; Swarts, J. C.; Conradie, J.; Leipoldt, J. G. *Acta Crystallogr.* **1993**, *49*, 82. (b) Conradie, J.; Lamprecht, G. J.; Otto, S.; Swarts, J. C. *Inorg. Chim. Acta* **2002**, *328*, 191.

(4) Swarts, P. J.; Immelman, M.; Lamprecht, G. J.; Greyling, S. E.; Swarts, J. C. *S. Afr. J. Chem.* **1997**, *50*, 208.

(5) (a) Swarts, J. C.; Swarts, D. M.; Maree, M. D.; Neuse, E. W.; La Madeleine, C.; van Lier, J. E. *Anticancer Res.* **2001**, *21*, 2033. (b) Swarts, J. C.; Vosloo, T. G.; Cronje, S. J.; du Plessis, W. C.; Van Rensburg, C. E. J.; Kreft, E.; Van Lier, J. E. *Anticancer Res.* **2008**, *28*, 2781. (c) Weber, B.; Serafin, A.; Michie, J.; Van Rensburg, C. E. J.; Swarts, J. C.; Baum, L. *Anticancer Res.* **2004**, *24*, 763.

(6) Du Plessis, W. C.; Erasmus, J. J. C.; Lamprecht, G. J.; Conradie, J.; Cameron, T. S.; Aquino, M. A. S.; Swarts, J. C. *Can. J. Chem.* **1999**, *77*, 378.

(7) (a) A. Auger, A.; Swarts, J. C. *Organometallics* **2007**, *26*, 102. (b) Davis, W. L.; Shago, R. F.; Langner, E. H. G.; Swarts, J. C. *Polyhedron* **2005**, *24*, 1611.

(8) Du Plessis, W. C.; Vosloo, T. G.; Swarts, J. C. *J. Chem. Soc., Dalton Trans.* **1998**, 2507.

(9) (a) Vosloo, T. G.; du Plessis, W. C.; Swarts, J. C. *Inorg. Chim. Acta* **2002**, *331*, 188. (b) Vosloo, T. G.; Swarts, J. C. *Trans. Met. Chem.* **2002**, *27*, 411. (c) Fourie, E.; Swarts, J. C.; Lorcy, D.; Bellec, N. *Inorg. Chem.* **2010**, *49*, 952.

(10) (a) Conradie, J.; Lamprecht, G. J.; Roodt, A.; Swarts, J. C. *Polyhedron* **2007**, *26*, 5075. (b) Conradie, J.; Swarts, J. C. *Organometallics* **2009**, *28*, 1018.

(11) (a) Maitlis, P. M.; Haynes, A.; Sunley, G. J.; Howard, M. J. *J. Chem. Soc., Dalton Trans.* **1996**, 2187. (b) Cavallo, L.; Sola, M. *J. Am. Chem. Soc.* **2001**, *123*, 12294. (c) Haynes, A.; Maitlis, P. M.; Morris, G. E.; Sunley, G. J.; Adams, H.; Badger, P. W.; Bowers, C. M.; Cook, D. B.; Elliot, P. I. P.; Ghaffer, T.; Green, H.; Griffin, T. R.; Payne, M.; Pearson, J. M.; Taylor, M. J.; Vickers, P. W.; Watt, R. J. *J. Am. Chem. Soc.* **2007**, *126*, 2847. (d) Jones, J. *Platinum Met. Rev.* **2000**, *44*, 94.

(12) Atwood, J. D. *Coord. Chem. Rev.* **1988**, *83*, 93.

(13) Gordy scale group electronegativities, χ_R, are empirical numbers that express the combined tendency of not only one atom, but a group of atoms, like R = CF_3 or ferrocenyl (Fc), to attract electrons (including those in a covalent bond) as a function of the number of valence electrons, *n*, and the covalent radius, *r* (in Å), of groups as discussed in (a) Wells, P. R. In *Progress in Physical Organic Chemistry*; John Wiley & Sons, Inc.: New York, 1968; Vol. *6*, pp 111−145 and (b) Kagarise, R. E. *J. Am. Chem. Soc.* **1955**, *77*, 1377.

(14) Conradie, J.; Swarts, J. C. *Dalton Trans.* **2011**, *40*, 5844.

(15) Conradie, J.; Swarts, J. C. *Eur. J. Inorg. Chem.* **2011**, 2439.

(16) (a) Taylor, M. J. In *Comprehensive Coordination Chemistry*; Wilkinson, G., Gillard, R. D., McCleverty, J. A., Eds.; Pergamon Press: Oxford, U.K., 1987; Vol. 3, pp 105−152.

(17) Chen, L.; Qiao, J.; Duan, L.; Qiu, Y. *Synth. Met.* **2007**, *157*, 713.

(18) Mazurenko, E.; Gerasimchuk, A. *J. Phys. (Paris)* **1995**, *C5*, 547.

(19) Helms, A. B.; Burgess, J. S.; Street, S. C. *Surf. Sci.* **2009**, *22*, 3262.

(20) Morgan, G. T.; Drew, H. D. K. *J. Chem. Soc.* **1921**, *119*, 1058.

(21) Mehrotra, R. C.; Rai, A. K. *Polyhedron* **1991**, *10*, 1967.

(22) Fortman, J. J.; Sievers, R. E. *Inorg. Chem.* **1967**, *6*, 2022.

(23) Bradley, D. C.; Mehrotra, R. C.; Rothwell, I. P.; Singh, A. In *Alkoxo and Aryloxo Derivatives of Metals*; Bradley, D. C., Ed.; Academic Press: New York, 2001; pp 117−119.

(24) (a) Fay, R. C.; Pepper, T. S. *J. Am. Chem. Soc.* **1962**, *84*, 2303. (b) Fay, R. C.; Pepper, T. S. *J. Am. Chem. Soc.* **1963**, *85*, 500.

(25) Zanello, P.; de Biani, F. F.; Glidewell, C.; Koenig, J.; Marsh, S. J. *Polyhedron* **1998**, *17*, 1795.

(26) Hill, M. G.; Lamanna, W. M.; Mann, K. R. *Inorg. Chem.* **1991**, *30*, 4687.

(27) (a) Swarts, J. C.; Nafady, A.; Roudebush, J. H.; Trupia, S.; Geiger, W. E. *Inorg. Chem.* **2009**, *48*, 2156. (b) Barriere, F.; Kirss, R. U.; Geiger, W. E. *Organometallics* **2005**, *24*, 48. (c) Barriere, F.; Camire, N.; Geiger, W. E.; Mueller-Westerhoff, U. T.; Sanders, R. *J. Am. Chem. Soc.* **2002**, *124*, 7262. (d) F. Barriere, F.; Geiger, W. E. *J. Am. Chem. Soc.* **2006**, *128*, 3980. (e) Nafady, A.; Chin, T. T.; Geiger, W. E. *Organometallics* **2006**, *25*, 1654. (f) Chong, D. S.; Slote, J.; Geiger, W. E. *J. Electroanal. Chem.* **2009**, *630*, 28.

(28) (a) Cook, M. J.; Chambrier, I.; White, G.; Fourie, E.; Swarts, J. C. *Dalton Trans.* **2009**, 1136. (b) Van Order, N.; Geiger, W. E.; Bitterwolf, T. E.; Reingold, A. L. *J. Am. Chem. Soc.* **1987**, *109*, 5680. (c) Pierce, D. T.; Geiger, W. E. *Inorg. Chem.* **1994**, *33*, 373. (d) Fourie, E.; Swarts, J. C.; Chambrier, I.; Cook, M. J. *Dalton Trans.* **2009**, 1145. (e) Geiger, W. E.; Van Order, N.; Pierce, D. T.; Bitterwolf, T. E.; Reingold, A. L.; Chasteen, N. D. *Organometallics* **1991**, *10*, 2403. (f) Kemp, K. C.; Fourie, E.; Conradie, J.; Swarts, J. C. *Organometallics* **2008**, *27*, 353.

(29) Smith, M. B.; March, J. *March's Advanced Organic Chemistry: Reactions, Mechanisms, and Structure*, 5th ed; John Wiley and Sons: New York, 2001; pp 20−36.

(30) Allen, F. H.; Kennard, O.; Watson, D. G.; Brammer, L.; Orpen, A. G.; Taylor, R. J. *J. Chem. Soc., Perkin Trans.* **1987**, *2*, S8.

(31) (a) Du Plessis, W. C.; Davis, W. L.; Cronje, S. J.; Swarts, J. C. *Inorg. Chim. Acta* **2001**, *314*, 97. (b) Von Chrzanowski, L. S.; Lutz, M.; Spek, A. L. *Acta Crystallogr.* **2006**, *E62*, m3318. (c) Von Chrzanowski, L. S.; Lutz, M.; Spek, A. L. *Acta Crystallogr.* **2007**, *C63*, m129.

(32) Gritzner, G.; Kuta, J. *Pure Appl. Chem.* **1984**, *56*, 461.

(33) Leading references describing the electrochemical activity and behavior of ferrocene and decamethylferrocene in a multitude of organic solvents are (a) I. Noviandri, I.; Brown, K. N.; Fleming, D. S.; Gulyas, P. T.; Lay, P. A.; Masters, A. F.; Phillips, L. *J. Phys. Chem. B* **1999**, *103*, 6713. (b) Connelly, N. G.; Geiger, W. E. *Chem. Rev.* **1996**, *96*, 877. (c) Ruiz, J.; Astruc, D. *C. R. Acad. Sci. (Paris), Ser. IIc 1* **1998**, 21. (d) Aranzaes, R. J.; Daniel, M. C.; Astruc, D. *Can. J. Chem.* **2006**, *84*, 288.

(34) Gericke, H. J.; Barnard, N. I.; Erasmus, E.; Swarts, J. C.; Cook, M. J.; Aquino, M. A. S. *Inorg. Chim. Acta* **2010**, *363*, 2222.

(35) (a) Evans, D. H.; O'Connell, K. M.; Peterson, R. A.; Kelly, M. J. *J. Chem. Educ.* **1983**, *60*, 290. (b) Kissinger, P. T.; Heineman, W. R. *J. Chem. Educ.* **1983**, *60*, 702. (c) Van Benshoten, J. J.; Lewis, L. Y.; Heineman, W. R. *J. Chem. Educ.* **1983**, *60*, 772. (d) Mobbott, G. A. *J. Chem. Educ.* **1983**, *60*, 697.

(36) Conradie, J.; Cameron, T. S.; Aquino, M. A. S.; Lamprecht, G. J.; Swarts, J. C. *Inorg. Chim. Acta* **2005**, *358*, 2530.

(37) Auger, A.; Muller, A. J.; Swarts, J. C. *Dalton Trans.* **2007**, 3623.

(38) Shago, R. F.; Swarts, J. C.; Kreft, E.; Van Rensburg, C. E. J. *Anticancer Res.* **2007**, *27* (5a), 3431.

(39) Liu, A.; Leese, D. N.; Swarts, J. C.; Sykes, A. G. *Inorg. Chim. Acta* **2002**, *337*, 83.

(40) (a) Swarts, J. C.; Aquino, M. A. S.; Lam, K.-Y.; Sykes, A. G. *Biochim. Biophys. Acta* **1995**, *1247*, 215. (b) Swarts, J. C.; Sykes, A. G. *Anti-Cancer Drug Des.* **1994**, *9*, 41. (c) Han, J. Y.; Swarts, J. C.; Sykes, A. G. *Inorg. Chem.* **1996**, *35*, 4629. (d) Nyholm, S.; Thelander, L.; Gräslund, A. *Biochemistry* **1993**, *32*, 11569. (e) Artin, E.; Wang, J.; Lohman, G. J. S.; Yokoyama, K.; Yu, G.; Griffin, R. G.; Bar, G.; Stubbe, J. *Biochemistry* **2009**, *48*, 11622.

(41) Osella, D.; Ferrali, M.; Zanello, P.; Laschi, F.; Fontani, M.; Nervi, C.; Carvigiolio, G. *Inorg. Chim. Acta* **2000**, *306*, 42.

(42) Fourie, E.; Erasmus, E.; Swarts, J. C.; Jakob, A.; Lang, H.; Joone, G. K.; Van Rensburg, C. E. J. *Anticancer Res.* **2011**, *31*, 825.

(43) LeSuer, R. J.; Buttolph, C.; Geiger, W. E. *Anal. Chem.* **2004**, *76*, 6395.

(44) *Apex2* (Version 1.0-27); Bruker AXS Inc.: Madison, WI, 2005.

(45) *COSMO* (Version 1.48); Bruker AXS Inc.: Madison, WI, 2003.

(46) *SAINT-Plus including XPREP* (Version 7.12); Bruker AXS Inc.: Madison, WI, 2004.

(47) *SADABS* (Version, 2004/1); Bruker AXS Inc.: Madison, WI, 1998.

(48) Altomare, A.; Burla, M. C.; Camalli, M.; Cascarano, G. L.; Giacovazzo, C.; Guagliardi, A.; Moliterni, G. G.; Polidori, G.; Spagna, R. *J. Appl. Crystallogr.* **1999**, *32*, 115.

(49) Farrugia, L. J. *J. Appl. Crystallogr.* **1999**, *32*, 837; WinGX1.70.01.

(50) Sheldrick, G. M. *SHELXL97, Program for Crystal Structure Refinement*; University of Göttingen: Göttingen, Germany, 1997.

(51) Brandenburg, K.; Putz, H. *DIAMOND*, Release 3.1a; Crystal Impact GbR: Bonn, Germany, 2005.

(52) *SQUEEZE*; Van der Sluis, P.; Spek, A. L. *Acta Crystallogr.* **1990**, *A46*, 194.